Received: 10 December 2019 | Revised: 15 July 2020 | Accepted: 12 August 2020

DOI: 10.1002/ijc.33268

IJC International Journal of Cancer

MOLECULAR CANCER BIOLOGY

miR-34a is upregulated in *AIP*-mutated somatotropinomas and promotes octreotide resistance

Eva-Maria Bogner[1] | Adrian F. Daly[2] | Sebastian Gulde[1] | Auli Karhu[3] | Martin Irmler[4] | Johannes Beckers[4,5,6] | Hermine Mohr[1] | Albert Beckers[2] | Natalia S. Pellegata[1]

[1]Institute for Diabetes and Cancer, Helmholtz Zentrum München, Neuherberg, Germany

[2]Department of Endocrinology, Centre Hospitalier Universitaire de Liège, Liège Université, Liège, Belgium

[3]Department of Medical and Clinical Genetics & Genome-Scale Biology Research Programs Unit, University of Helsinki, Helsinki, Finland

[4]Institute of Experimental Genetics, Helmholtz Zentrum München, Neuherberg, Germany

[5]Technische Universität München, Chair of Experimental Genetics, Freising, Germany

[6]German Center for Diabetes Research (DZD), Neuherberg, Germany

Correspondence
Natalia S. Pellegata, Institute for Diabetes and Cancer, Helmholtz Zentrum München, Ingolstaedter Landstrasse 1, 85764 Neuherberg, Germany.
Email: natalia.pellegata@helmholtz-muenchen.de

Funding information
Deutsche Forschungsgemeinschaft, Grant/Award Number: TRR 205/B11; Deutsche Krebshilfe, Grant/Award Number: 70112383;

Abstract

Pituitary adenomas (PAs) are intracranial tumors associated with significant morbidity due to hormonal dysregulation, mass effects and have a heavy treatment burden. Growth hormone (GH)-secreting PAs (somatotropinomas) cause acromegaly-gigantism. Genetic forms of somatotropinomas due to germline *AIP* mutations (*AIP*mut+) have an early onset and are aggressive and resistant to treatment with somatostatin analogs (SSAs), including octreotide. The molecular underpinnings of these clinical features remain unclear. We investigated the role of miRNA dysregulation in *AIP*mut + vs *AIP*mut− PA samples by array analysis. miR-34a and miR-145 were highly expressed in *AIP*mut+ vs *AIP*mut− somatotropinomas. Ectopic expression of *AIP*mut (p.R271W) in $Aip^{-/-}$ mouse embryonic fibroblasts (MEFs) upregulated miR-34a and miR-145, establishing a causal link between *AIP*mut and miRNA expression. In PA cells (GH3), miR-34a overexpression promoted proliferation, clonogenicity, migration and suppressed apoptosis, whereas miR-145 moderately affected proliferation and apoptosis. Moreover, high miR-34a expression increased intracellular cAMP, a critical mitogenic factor in PAs. Crucially, high miR-34a expression significantly blunted octreotide-mediated GH inhibition and antiproliferative effects. miR-34a directly targets *Gnai2* encoding Gαi2, a G protein subunit inhibiting cAMP production. Accordingly, Gαi2 levels were significantly lower in *AIP*mut+ vs *AIP*mut− PA. Taken

Abbreviations: 3′UTR, 3′-untranslated region; AB, avidin-biotin; AC, adenylate cyclase; ACTH, adrenocorticotropic hormone; AHR, aryl hydrocarbon receptor; AIP, aryl hydrocarbon receptor-interacting protein; *AIP*mut-, *AIP* mutation-negative; *AIP*mut+, *AIP* mutation-positive; AML, acute myeloid leukemia; ANOVA, analysis of variance; B2m, β2-microglobulin; cAMP, cyclic adenosine monophosphate; cDNA, complementary DNA; CHX, cycloheximide; CLL, chronic lymphocytic leukemia; CO2, carbon dioxide; Ct, threshold cycle; DMEM, Dulbecco's Modified Eagle's Medium; DNA, deoxyribonucleic acid; dNTP, nucleoside triphosphate; DTT, dithiothreitol; ELISA, enzyme-linked immunosorbent assay; EPOX, epoxomycin; ERK1/2, extracellular signal-regulated kinases 1/2; FBS, fetal bovine serum; FC, fold change; FDR, false discovery rate; FFPE, formalin-fixed, paraffin-embedded; FIPA, familial isolated pituitary adenoma; GEO, Gene Expression Omnibus; GH, growth hormone; GNAI, G-protein inhibitory alpha subunit; GO, Gene Ontology; GPR101, G-protein coupled receptor 101; Gαi, G-protein inhibitory alpha subunit; HEK293, human embryonic kidney 293 cells; HS, horse serum; Hsp90, heat shock protein 90; Igf-1, insulin-like growth factor 1; IHC, immunohistochemistry; IPA, Ingenuity Pathway Analysis; Magmas, Mitochondria-associated granulocyte-macrophage CSF-signaling molecule; MEF *AIP*−/−, AIP knockout mouse embryonic fibroblasts; MEF, mouse embryonic fibroblasts; MEN1, multiple endocrine neoplasia type 1; MEN4, multiple endocrine neoplasia type 4; miRNA, microRNA; mRNA, messenger RNA; mTOR, mechanistic target of rapamycin; n.s., not significant; NFPA, nonfunctioning pituitary adenoma; Oct, octreotide; oncomiR, oncogenic miRNA; PA, pituitary adenoma; Pam16, presequence translocase-associated motor 16; PBS, phosphate-buffered saline; PCR, polymerase chain reaction; PDE, phosphodiesterase; pen/strep, penicillin-streptomycin; pERK1/2, phosphorylated ERK1/2; PLAG1, pleomorphic adenoma gene 1; PRKCD, protein kinase Cδ; qRT-PCR, quantitative real-time PCR; RIPA, radioimmunoprecipitation assay; RNA, ribonucleic acid; RNase, ribonuclease; SDS-PAGE, sodium dodecyl sulfate-polyacrylamide gel electrophoresis; SEM, standard error of the mean; SSA, somatostatin analog; SSTR, somatostatin receptor; TBP, TATA-binding protein; tMF, transformed mycosis fungoides; TPR, tetratricopeptide repeat; TPT1, translationally controlled tumor protein; TSH, thyroid-stimulating hormone; Wst-1, water-soluble tetrazolium; wt, wild-type; X-LAG, X-linked acrogigantism.

Correction added on 05 October 2020,after first online publication: Projekt Deal funding statement has been added.

Fonds d'Investissement Pour la Recherche Scientifique; Helmholtz Alliance; JABBS Foundation

together, somatotropinomas with *AIP* mutations overexpress miR-34a, which in turn downregulates Gαi2 expression, increases cAMP concentration and ultimately promotes cell growth. Upregulation of miR-34a also impairs the hormonal and antiproliferative response of PA cells to octreotide. Thus, miR-34a is a novel downstream target of mutant *AIP* that promotes a cellular phenotype mirroring the aggressive clinical features of *AIP*mut+ acromegaly.

KEYWORDS

aryl hydrocarbon receptor-interacting protein, G protein subunit alpha i2, miR-34a, octreotide resistance, pituitary adenoma

1 | INTRODUCTION

Pituitary adenomas (PAs) comprise up to 15% of intracranial tumors and clinically relevant PAs occur in approximately 1:1000 of the general population.[1,2] They represent a challenging health burden due to disordered hormonal function and tumor growth; PA treatments are invasive, costly and require significant expertise.[3] PAs usually occur sporadically but about 5% of cases present as part of hereditary syndromes, like familial isolated pituitary adenomas (FIPA), multiple endocrine neoplasia type 1 and 4 (MEN1, MEN4), Carney complex, McCune-Albright syndrome and X-linked acrogigantism.[4-7] Mutations of the *aryl hydrocarbon receptor-interacting protein* (*AIP*) gene (*AIP*mut) account for 15%-20% of FIPA kindreds and are particularly important in the pathogenesis of pediatric-onset PAs.[8,9]

Germline *AIP*mut-associated (*AIP*mut+) PAs are distinctive, presenting usually as growth hormone (GH)-secreting PAs (somatotropinomas) that are significantly larger, more invasive and occur at a younger age than PAs without *AIP* mutations (*AIP*mut-).[10] The first-line treatment for sporadic somatotropinomas is transsphenoidal surgery, which controls hormone hypersecretion in only about 50% of patients.[11] For uncontrolled or recurrent disease, medical therapy with somatostatin analogs (SSA) is used in most cases.[12] As the response to SSA is dependent on several molecular determinants, 10%-30% of patients do not respond to this therapy and can require other therapies such as pegvisomant or radiotherapy; novel therapeutic approaches (eg, metformin and statins) are now being evaluated preclinically and in small patient cohorts (reviewed in Reference 13). *AIP*mut + somatotropinomas are relatively resistant to first-line medical treatment with SSA.[10] The molecular pathways that lead to this aggressive, treatment-resistant phenotype are of great clinical relevance, but the specific pathway(s) are unclear. AIPmut+ leads to impaired interaction with phosphodiesterase-4A5 (PDE4A5),[14] dysregulated protein kinase A (PKA) function,[15,16] and disrupted regulation of the inhibitory G protein, Gαi2, which can increase cyclic adenosine monophosphate (cAMP).[17,18]

Like many other human tumor types, the development of PAs can be influenced by microRNAs (miRNAs); differential miRNA expression in PAs is related to histological tumor subtypes, clinical behavior and treatment responses.[19-24] Interactions between miRNAs and normal, non-mutated AIP have also been noted: miR-107 is overexpressed in somatotropinomas and binds to and represses AIP in GH3 cells in vitro.[25] As the effects of *AIP*mut per se on miRNA expression in human tumors are unknown, we set out to determine the miRNA signature of *AIP*mut+ and *AIP*mut− PAs. Among the miRNAs we identified as being upregulated in *AIP*mut+ PA tissues was miR-34a. We show that miR-34a has pro-oncogenic functions in PAs, likely mediated by increased cyclic adenosine monophosphate (cAMP) signaling, and that Gαi2 is a direct target of miR-34a and is differentially expressed in human PAs depending on *AIP*mut status. We report for the first time that miR-34a upregulation leads not only to increased cell proliferation and GH secretion in vitro, but also induces resistance to the antiproliferative and hormonal effects of the first-generation somatostatin analog, octreotide.

What's new?

Germline mutations in the *AIP* gene are a significant cause of inherited intracranial pituitary adenoma (PA). *AIP* mutation-positive (*AIP*mut+) PAs are characterized by early tumor onset, aggressive tumor behavior, and resistance to somatostatin analogs (SSAs). Here, the microRNA-34a (miR-34a) was found to be upregulated in *AIP*mut+ PA, where it correlates with pro-oncogenic features, high cAMP levels, and impaired response to octreotide, a first-generation SSA. In vitro, miR-34a directly targeted *GNAI2*, the gene encoding Gαi2, an inhibitor of cAMP synthesis known to be downregulated in *AIP*mut+ adenomas. Together, miR-34a and Gαi2 may be valuable biomarkers for therapeutic stratification of *AIP*mut+ patients.

2 | MATERIALS AND METHODS

2.1 | Patient samples

For the current study, a total of 42 primary PAs were collected comprising 32 somatotropinomas and 10 prolactinomas. Twenty somatotropinomas were negative for *AIP*mut (*AIP*mut−) and 12 were *AIP*mut+. Three prolactinomas were *AIP*mut+and seven were *AIP*mut−.

TABLE 1 Summary of the clinical characteristics of the PA patients that participated in the study

	Number of patients (n = 42)		*AIP*mut− (n = 27)		*AIP*mut+ (n = 15)	
	n	%	n	%	n	%
Sex						
Female	20	48	17	63	3	20
Male	22	52	10	37	12	80
Age at diagnosis						
<30 years	20	48	6	22	14	93
≥30 years	22	52	21	78	1	7
Tumor size						
Micro	8	19	8	30	0	0
Macro	30	71	17	63	13	87
Giant	4	10	2	7	2	13
Invasion						
No	21	50	17	63	4	27
Yes	21	50	10	37	11	73

For miRNA array analysis, 22 PAs were used (10 *AIP*mut− and 12 *AIP*mut+). Among these samples, there were 12 somatotropinomas (5 *AIP*mut− and 7 *AIP*mut+). A summary of the clinical characteristics of the patients is reported in Table 1 and a list of the clinical features, mutation status and the presence of LOH is provided in Table S1. In line with previous results, the age at diagnosis was significantly lower (Figure S1A) and the tumor size was significantly larger (Figure S1B) in *AIP*mut+ compared to *AIP*mut− patients.

2.2 | RNA extraction and processing

RNA was extracted from the patient samples with the RNeasy Mini Kit (#74104, Qiagen) and RNA concentration was determined by a Spectrophotometer NanoDrop ND-1000 (Thermo Fisher Scientific, Waltham, Massachusetts).

2.3 | DNA extraction and LOH analysis

To establish germline *AIP* status, DNA was isolated from peripheral blood leukocytes and *AIP* was sequenced under conditions described.[8-10] Germline DNA was also studied for deletions in *AIP* using multiplex ligand-dependent probe amplification (MLPA), but no germline deletions were present. DNA was also extracted following microdissection of FFPE tissue sections of pituitary adenomas and evidence of allelic loss to demonstrate loss of heterozygosity (LOH) was performed using MLPA (SALSA P244 probemix, MRC-Holland, The Netherlands).

2.4 | Microarray hybridization and data analysis

RNA samples were analyzed by the GeneChip miRNA 1.0 array (Affymetrix/Thermo Fisher Scientific.), which is based on the Sanger miRBase miRNA database v11 (April 15, 2008). Tumor tissue was isolated from previously identified FFPE tissue sections with the RNeasy FFPE Kit (#73504, Qiagen). Total RNA (250 ng) was labeled with the FlashTag Biotin HSR kit (Genisphere) and hybridized. Staining and scanning were done according to the Affymetrix expression protocol. Array data was processed and annotated with the miRNA QC tool (Affymetrix, version 1.0.33.0) using settings recommended by Genisphere. Briefly, background was detected and removed by RMA global background correction, followed by quantile normalization and summarization using median polishing. Statistical analysis of the resulting dataset was performed by utilizing the statistical programming environment R (R Development Core Team 2011 R: A Language and Environment for Statistical Computing. Vienna, Austria: The R Foundation for Statistical Computing) implemented in CARMAweb.[26] Genewise testing for differential expression was done employing the limma *t*-test and Benjamini-Hochberg multiple testing correction. All gene sets were filtered for true detection in at least half of the samples in at least one group per comparison. For technical replicates, the average was used for calculations. Functional annotations were generated through the use of QIAGEN's Ingenuity Pathway Analysis (IPA, QIAGEN Redwood City, www.qiagen.com/ingenuity) using Fisher's exact test *P* values. Input was regulated eight miRNAs from somatotropinomas (FC > 1.5x, $P < .002$; miR-383 was excluded). Heat maps were generated in R.

2.5 | Plasmid constructs and antibodies

The p.R271W mutation was introduced by site-directed mutagenesis (QuikChange II Site-Directed Mutagenesis Kit, #200523, Agilent Technologies) in the wild-type human *AIP* cDNA cloned in a pCMV-Myc backbone. The mutagenesis was verified by sequencing.

A fragment containing the predicted seed match and the mutated seed match of miR-34a in the rat 3′UTR of the GNAI2 gene was generated by annealing two oligos that represent the top and bottom

strand of the fragment. After oligo annealing, the fragments were cloned in a psiCHECK-2 backbone (#C8021, Promega).

Primers and Oligos for cloning and mutagenesis are listed in Table S2.

Primary antibodies are listed in Table S3.

2.6 | Quantitative real-time polymerase chain reaction

RNA was extracted using RNeasy Mini Kit (#74104, Qiagen) or with the Maxwell 16 LEV simplyRNA Purification Kit (#AS1270, Promega) following the manufacturer's instructions. Quantitative real-time polymerase chain reaction (qRT-PCR) was performed using TaqMan inventoried primers and probes (Applied Biosystems, Foster City, California) for the indicated genes, as described previously.[27]

The differential expression of selected miRNAs was validated by qRT-PCR. RNA was isolated using the miRNeasy Mini Kit (#217004, Qiagen) and miRNA concentration was determined as described before. Synthesis of cDNA was performed by TaqMan miRNA Reverse Transcription Kit (#4366596, Applied Biosystems) and primer sets for the respective miRNAs (Applied Biosystems). For qRT-PCR miRNA primer sets (Applied Biosystems) for the indicated miRNAs were used. All reactions were performed in triplet PCR reactions with U6 snRNA (#4427975, Applied Biosystems) as an endogenous control using a comparative Ct method.

2.7 | Cell culture and transient transfections

GH3 cells (RRID:CVCL 0273; *Rattus norvegicus* mixed GH-prolactin secreting PA cell line), MEFs from AIP knockout mice (MEF AIP −/−) (RRID:CVCL UJ02), HEK293 cells (RRID:CVCL 0045) and GH4C1 cells (RRID:CVCL 0276) clone of GH3 with little or no detectable levels of growth hormone) were maintained in culture as described in Table S4. Cell lines were purchased by LGC Promochem, whereas AIP−/− MEFs were established in the laboratory of A. Karhu. All miRNA mimics used and inhibitors with respective controls are listed in Table S5.

MEF AIP −/− were transiently transfected with AIP plasmids and co-transfected with AIP plasmids and miRNA hairpin inhibitors (25 nM) with the 4D-Nucleofector System X unit (Lonza Group AG) and the P4 Primary Cell 4D-Nucleofector X Kit L (#V4XP-4012, Lonza Group AG). Electroporation was conducted using the pulse code CZ-167.

GH3 cells were transiently transfected with 150 nM miRNA mimics (miRIDIAN unspecific control mimic; miRIDIAN microRNA rat rno-miR-34a mimic; miRIDIAN microRNA rat rno-miR-145 mimic, from Dharmacon) or hairpin inhibitors (miRIDIAN microRNA rat rno-miR-34a inhibitor, from Dharmacon) using the 4D-Nucleofector System X unit and the SF Cell Line 4D-Nucleofector X Kit L (#V4XC-2012, Lonza Group AG). Electroporation was conducted using the pulse code DS-131.

HEK293 cells were authenticated within the last 3 years by DSMZ (Braunschweig) using short tandem repeat profiling. HEK293 cells were plated 24 hours before transfection in 24-well-plates at a density of 0.05×10^6 cells per well. The cells were transiently transfected with Lipofectamine 3000 Transfection Reagent (#L3000015, Thermo Fisher Scientific Inc.) according to the manufacturer's instructions with 1 μg of the vector and 150 nM of either negative control inhibitor or anti-miR-34a.

All cell lines were routinely tested for mycoplasma contamination using the PCR Mycoplasma Test Kit (#PK-CA91-1048, PromoKine) and found to be mycoplasma-free.

2.8 | Drug treatments

Cells were treated with 25 μg/mL cycloheximide (#C4859, Sigma-Aldrich) and 10 μM epoxomycin (EPOX, #BML-PI127-0100, Enzo Life Sciences) in complete medium for the indicated times.

For therapy response, cells were treated with 10 or 100 nM octreotide (kindly provided by Italfarmaco SpA) in serum-free medium for the indicated times.

2.9 | Protein extraction and Western blotting

Cells were collected at the indicated time points and lysed in radioimmunoprecipitation assay (RIPA) buffer (#R0278, Sigma-Aldrich) supplemented with protease (#04693124001, Roche Diagnostics) and phosphatase inhibitors (#04906845001, Roche Diagnostics). Protein concentrations were determined by the Pierce BCA Protein Assay Kit (#23225, Thermo Fisher Scientific Inc.). Equal protein amounts were separated on 10% SDS-PAGE gels. Antibodies were applied at 4°C overnight incubation (primary antibody) and 1-hour incubation (secondary antibody) at room temperature. Proteins were visualized by the SuperSignal West Pico Chemiluminescent Substrate Kit (#34080, Thermo Fisher Scientific Inc.).

2.10 | Functional characterization of transfected cells

Cell viability was assessed by a colorimetric assay using Wst-1 reagent according to the manufacturer's recommendations (#11644807001, Roche, La Roche Ltd).

Migration assays were performed using 24-well plates with uncoated polycarbonate membrane inserts (#353097, BD Biosciences). Cells were allowed to migrate for 24 hours. Membranes were stained by 1.5% (w/v) Toluidin Blue (#115930, Merck), fixed with Methanol (#106009, Merck) and mounted on glass slides with Pertex mounting medium (#41-4010-00, MEDITE GmbH). Images were recorded using an Olympus BX43 microscope.

Clonogenic potential of the cells was monitored by seeding the miRNA overexpressing cells at a low density of 1×10^3 cells per well in six-well plates. After 8 days, colonies were stained with 0,3% Crystal Violet in 30% ethanol and those with a diameter >100 μm were counted.

GH3 cells transfected with miRNA mimics were plated in 96-well plate at a density of 1.5×10^5 cells per well and six wells per group. For assessment of apoptosis in the cells, Caspase-Glo 3/7 Assay (#G8090, Promega) was performed according to the manufacturer's instructions.

2.11 | Immunoassays

Transfected GH3 cells (7×10^5 per well) were plated in six-well plates and 24 hours later, cAMP levels were determined by using an ELISA kit (#ADI-900-006, Enzo Life Sciences) according to the manufacturer's protocol.

After transfection GH3 cells were plated at a density of 8×10^4 cells per well in a 24-well plate in serum-free medium. After 24 hours, cells were treated with 100 nM Octreotide for additional 48 hours. The supernatant was then collected and GH was measured using a Rat/Mouse ELISA Kit (#EZRMGH-45K, Merck Millipore) whereas prolactin was measured with the rat ELISA Kit (#589701, Cayman Chemical).

2.12 | miRNA target prediction

The targets of the differentially expressed miRNAs were predicted by four different prediction tools, TargetScan 7.0, miRANDA-mirSVR, DIANA tools and PITA that take different parameters into consideration (Table S6).

2.13 | Reporter gene assays

To conduct reporter gene assays, HEK293 cells were lysed 24 hours after transfection according to the protocol of the Dual-Luciferase Reporter (DLR) Assay Kit (#E1980, Promega). Subsequently the reporter assay was performed according to the manufacturer's instructions.

2.14 | Immunohistochemistry and scoring

Immunhistochemical stainings were performed on an automated immunostainer (Ventana Medical Systems) as previously described.[28] Primary antibodies were diluted in Dako REALTM antibody diluent (Dako). Positive controls were included in each run. The slides were counterstained with hematoxylin for 10 seconds and washed under running water for 4 minutes. Images were recorded using an Olympus BX43 microscope (Olympus).

For Gαi-2-immunohistochemistry (IHC) an Avidin-Biotin block (AB-block) was used to decrease unspecific background staining. For AIP-IHC the AB-block was not necessary.

IHC results were evaluated using a semiquantitative method that assessed the staining intensity: – (negative), + (mild), ++ (moderate) and +++ (strong). Slides were scored using a double-blind method by two independent observers; the percentage of discrepancies was below 3%. Images were recorded using a Hitachi camera HW/C20 installed in a Zeiss Axioplan microscope with Intellicam software (Carl Zeiss MicroImaging).

2.15 | Statistical analysis

Results of the cell assays are shown as the mean of values obtained in independent experiments ± SEM. Unpaired two-tailed Student's *t*-test, Mann-Whitney test, one-way and two-way ANOVA were used to detect significance between two series of data, and $P < .05$ was considered statistically significant.

3 | RESULTS

3.1 | miRNA expression analysis in *AIP*mut+ *vs* *AIP*mut− adenomas

Eighteen PAs were used for miRNA profiling (Figure S2) using GeneChip miRNA arrays. In somatotropinomas, nine miRNAs were differentially expressed ($P < .002$) in *AIP*mut+ compared to *AIP*mut− tumors and showed a >1.5-fold change in expression. Six of them (miR-187, miR-383, miR-145, miR-34a, miR-143, miR-1231) were significantly upregulated and three (miR-195, miR-497, miR-26a) downregulated in *AIP*mut+ vs *AIP*mut− (Figure 1A). In prolactinomas, three miRNAs were regulated using the same criteria (Figure S3). One *AIP*mut+ prolactinoma was excluded due to suboptimal RNA quality, and since only two samples remained, we focused on the somatotropinomas for subsequent analyses. Some of the significant differentially expressed miRNAs have previously been linked to PAs, including miR-26a, downregulated in prolactinomas *vs* normal pituitary and upregulated in invasive adenomas[19,29]; miR-143 and miR-145 were downregulated in ACTH-secreting adenomas *vs* normal pituitary,[19] and miR-383, downregulated in invasive NFPAs.[19] To obtain a functional annotation of the differentially expressed miRNAs, we used Ingenuity Pathway Analysis. The most enriched terms were cancer-related, followed by terms related to cell cycle and cellular movement (Table S7), further supporting a role for the differentially expressed miRNAs in tumors. To validate the miRNA array results, we assessed the miRNAs with the highest differential expression (ie, miR-187, miR-383, miR-145, miR-34a and miR-195) by quantitative qRT-PCR in somatotropinoma samples. These analyses confirmed a significant upregulation of miR-187, miR-145 and miR-34a and a downregulation of miR-195 in *AIP*mut+ vs *AIP*mut− somatotropinomas (Figure 1B-F), whereas the differential expression of miR-383 could not be validated.

3.2 | Effects of mutant AIP in MEFs of *Aip*$^{-/-}$ mice

Given that the *AIP*-R271W mutation was predominant in our cohort (and is the most frequent missense *AIP*mut reported) we focused on

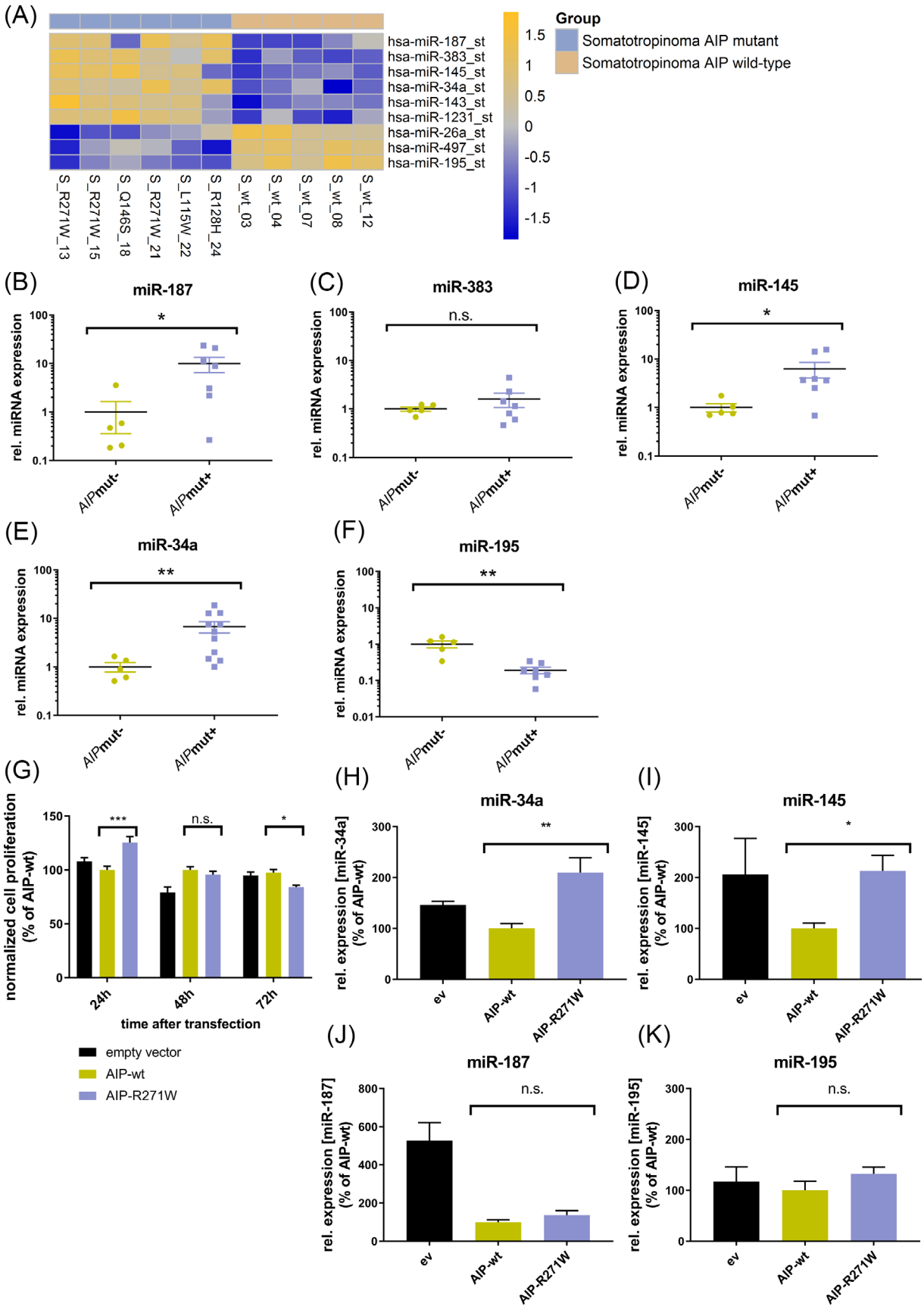

FIGURE 1 Legend on next page.

this mutated AIP protein. We first determined whether ectopic expression of the AIP-R271W variant affects cell proliferation. To avoid interference from endogenous wild-type AIP, MEFs from *Aip*$^{-/-}$ mice were transfected with AIP wild-type (wt) or AIP-R271W and cell proliferation was measured 24, 48 and 72 hours later. At the 24 hours time point, AIP-R271W increased cell proliferation vs AIP-wt (Figure 1G). This effect was no longer present 48 hours after transfection (Figure 1G). Western blot analysis revealed that the AIP-R271W protein was detectable only up to 24 hours after transfection, while AIP-wt was present throughout the duration of the experiment, suggesting that mutant AIP is less stable. Treatment of transfected cells with cycloheximide (CHX) confirmed this hypothesis: while AIP-wt showed no decrease up to 20 hours post-transfection, the level of AIP-R271W started to decrease already after 4 hours (Figure S4A). Treatment of transfected MEFs with both CHX and the proteasome inhibitor epoxomycin (EPOX) established that the degradation of mutant AIP is mediated, at least in part, by the proteasome (Figure S4B). This is in agreement with previously reported in vitro data analyzing the half-life of various *AIP*mut, including R271W.[30] Therefore, all subsequent experiments were conducted 24 hours after transfection and plasmid DNA was adjusted to reach equal protein levels for AIP-wt and AIP-R271W. Taken together, the ectopic expression of AIP-R271W promoted the proliferation of *Aip*$^{-/-}$ MEFs despite being present at low levels.

3.3 | Regulation of miRNA expression by mutant AIP in *Aip*−/− MEFs

To demonstrate a direct link between the presence of mutant AIP and differential miRNA expression, *Aip*$^{-/-}$ MEFs were transiently transfected with AIP-wt or AIP-R271W and the levels of selected differentially expressed miRNAs were assessed by qRT-PCR. In line with the array analyses, miR-34a and miR-145 were significantly upregulated upon transfection of AIP-R271W *vs* AIP-wt (Figure 1H,I). In contrast, the level of expression of miR-195 and miR-187 was similar in both conditions (Figure 1J,K). Thus, miR-34a and miR-145 were chosen for further in vitro characterization.

3.4 | Short-term upregulation of miR-145 and miR-34a promotes oncogenic features in PA cells

We next investigated whether upregulation of miR-34a and/or miR-145 (mimicking *AIP*mut+ tumors) affects the phenotypic features of PA cells. GH3 cells (derived from a rat GH/prolactin-secreting adenoma) were transfected with specific mimics for mature miR-34a and miR-145, and functional assays were performed assessing proliferation, clonogenic potential, migration and apoptosis (Figure 2A-D). Short-term overexpression of both miRNA mimics (24 hours) increased GH3 cell proliferation when compared to cells transfected with an unspecific control miRNA mimic (Figure 2A). GH3 cells overexpressing miR-34a migrated significantly more than the control ones, whereas transfection of miR-145 mimic had no effect on cell migration (Figure 2B). miR-34a and miR-145 overexpression decreased GH3 cells apoptosis, with miR-34a having the stronger effect (Figure 2D). miR-34a, but not miR-145, upregulation increased by 2-fold the clonogenic potential of GH3 cells *vs* cells transfected with unspecific miRNA control (Figure 2C). Altogether, high levels of miR-34a increased proliferation, clonogenicity, migration and suppressed apoptosis of PA cells. miR-145 upregulation only moderately promoted proliferation and decreased apoptosis.

3.5 | miR-34a but not miR-145 overexpression impairs the response to octreotide

Acromegaly and gigantism patients carrying AIP mutations poorly respond to somatostatin receptor subtype 2 (SST2)-specific SSAs such as octreotide and lanreotide; consequently, GH normalization and tumor shrinkage are limited in *AIP*mut+ -related acromegaly when compared to *AIP*mut− patients.[10] Given that mutated AIP upregulates miR-34a and miR-145, we assessed whether the levels of these miRNAs affect the ability of PA cells to respond to octreotide. GH3 cells were transfected with miRNA mimics as above, treated with octreotide for 72 hours and then cell proliferation was measured. Cells overexpressing the unspecific miRNA control and treated with octreotide showed decreased proliferation (−37%) *vs* untreated cells (Figure 2E), as previously reported.[31,32] A comparable reduction in cell proliferation was also observed in cells overexpressing miR-145 and treated with octreotide (−49%), whereas no suppression of cell proliferation was detected upon miR-34a upregulation (Figure 2E). This suggests that high miR-34a levels abolished the octreotide-dependent inhibition of PA cell proliferation.

Octreotide suppresses GH and prolactin (PRL) secretion from GH3 cells in vitro.[32] Overexpression of AIP-wt in GH3 cells reduces GH secretion by decreasing cAMP levels.[33] Thus, we measured GH in the supernatant of GH3 cells transfected with the above miRNA

FIGURE 1 miRNA expression profiles of AIPmut− and AIPmut+ PAs and validation. A, Heat map of the most differentially expressed miRNAs ($P < .002$, fold-change > 1.5x) in somatotropinomas (n = 11). Yellow (blue) indicates higher (lower) expression level (z-scales to mean expression per row). B-F, Validation of selected miRNAs in human somatotropinomas by qRT-PCR. The line represents the mean value and results are reported as the mean ± SEM. Each dot represents an AIPmut− PA, each filled square represents an AIPmut+ PA. *$P < .05$; **$P < .01$; n.s., not significant (by Mann-Whitney test). G, Aip−/− MEFs were transfected with empty vector, AIP-wt or AIP-R271W constructs. Cell viability was assessed 24, 48 and 72 hours after transfection. The experiment was independently performed three times each with six technical replicates and values are reported as the mean ± SEM. Only the statistical differences between AIP-wt and AIP-R271W are indicated. *$P < .05$; ***$P < .001$; n.s., not significant (by two-way ANOVA). H-K, Aip−/− MEFs were transfected with empty vector, AIP-wt or AIP-R271W constructs. Expression levels of selected miRNAs were measured 24 hours post-transfection. The experiments were performed with 2 to 4 biological and 2 to 3 technical replicates and results are reported (±SEM). *$P < .05$; **$P < .01$; n.s., not significant (by one-way ANOVA). Ev, empty vector

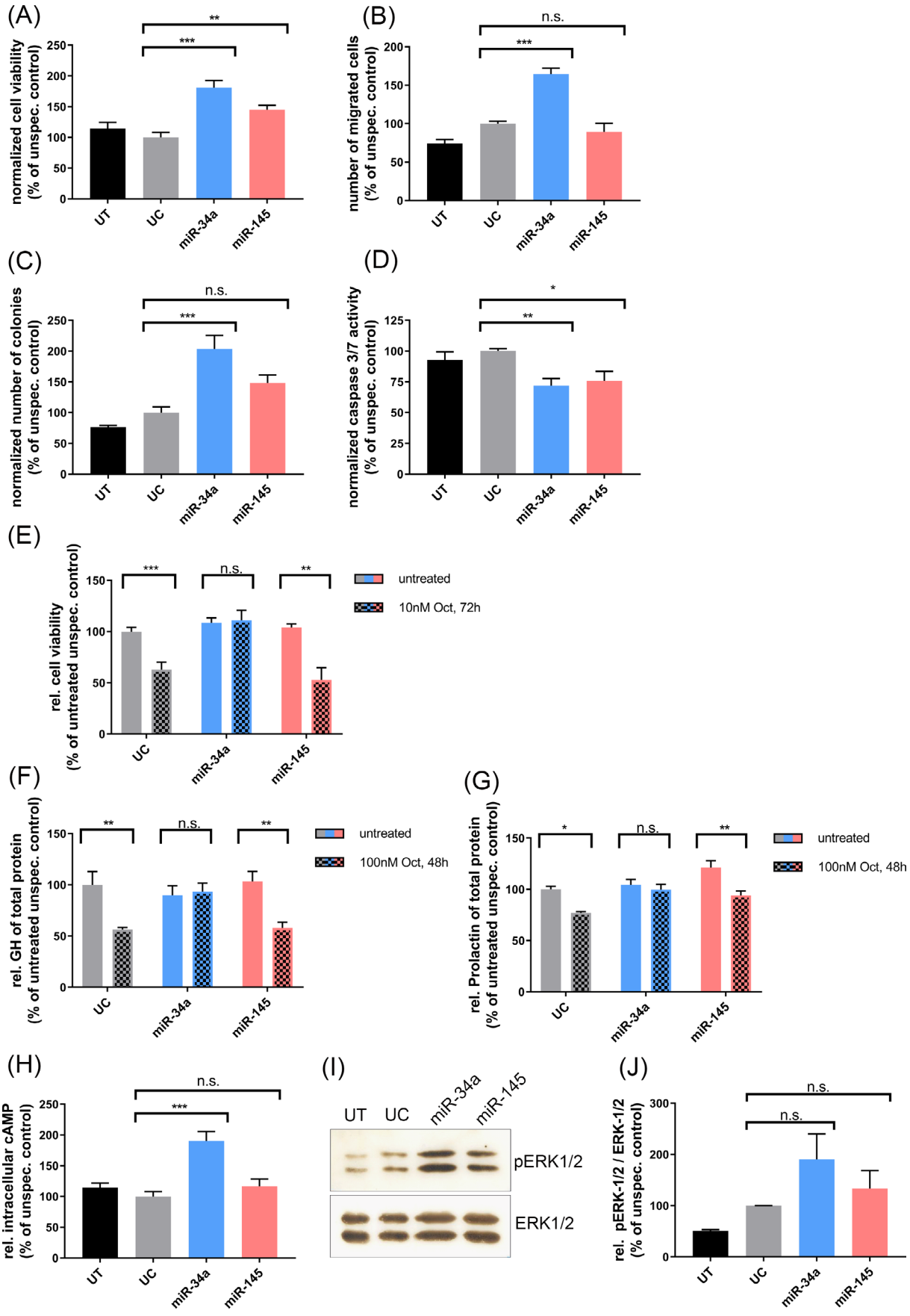

FIGURE 2 Legend on next page.

mimics and treated with octreotide for 48 hours (Figure 2F). For sake of completeness, we also measured PRL levels in the cells supernatant (Figure 2G). As expected, octreotide incubation led to a significant decrease in both GH and PRL secretion in cells transfected with the unspecific miRNA control (Figure 2F,G). A similar result was obtained in cells overexpressing miR-145 (−44% and −22%, respectively; Figure 2F,G). In contrast, upregulation of miR-34a led to a loss of octreotide-mediated suppression of both GH and PRL secretion (Figure 2F,G), indicating that high miR-34a levels mediated the lack of response of GH3 cells to octreotide treatment.

3.6 | Effects of the validated miRNAs on cAMP signaling in PA cells

Increased cAMP levels are an important hallmark of neuroendocrine tumors including PAs.[34] Moreover, cAMP signaling is dysregulated after AIP inactivation in mice and this associated with somatotrope tumorigenesis.[17] Therefore, we measured cAMP levels in GH3 cells transfected with miR-145 or miR-34a mimics, or with an unspecific miRNA control. Overexpression of miR-34a almost doubled the intracellular levels of cAMP in GH3 cells when compared to cells transfected with the unspecific negative control, whereas ectopic miR-145 expression had no effect on the amount of cAMP (Figure 2G).

cAMP has been reported to exert its mitogenic effect in somatotroph cells via phosphorylation of extracellular signal-regulated kinases (ERK1/2).[35,36] Therefore, we assessed total and phosphorylated ERK1/2 by western blotting. Overexpression of both miR-34a and miR-145 increased the levels of phosphorylated ERK1/2 compared to both untransfected and unspecific control-transfected cells (Figure 2H,I). The increase in phospho-ERK1/2 was more pronounced following miR-34a overexpression (*vs* miR-145) and this paralleled the higher intracellular levels of cAMP (Figure 2G).

3.7 | Guanine nucleotide-binding protein G(I) subunit alpha-2 (*GNAI2*) as a novel predicted target gene of miR-34a

*AIP*mut in PAs leads to upregulation of miR-34a, which in turn promotes proliferation and cAMP signaling. To better understand these effects, we identified predicted miR34a target genes using four different prediction tools (Table S6). Following the criteria outlined above (Materials and Methods), we selected several putative target genes (Table S8). As TargetScan considers only seed match and conservation for target prediction (Table S6), we excluded targets predicted only by algorithm alone. We focused on genes involved in cAMP signaling (Table S9), which included several phosphodiesterases (*PDE3a*, *PDE4A*, *PDE5a*, *PDE7b)* and G-protein alpha subunit family members (*GNAO1*, *GNAI2*, *GNAI3*, *GNAQ*; Table S9). *GNAI2* and *GNAI3* are interesting candidates as they encode inhibitory Gαi subunits which lead to decreased cAMP levels. To verify whether these genes were regulated by miR-34a, we transfected GH3 cells with the miR-34a mimic (for overexpression) or a specific anti-miR-34a (for downregulation) and assessed the level of *GNAI2* and *GNAI3*. The modulation of miR-34a levels were confirmed by qRT-PCR at 24 hours and 48 hours post-transfection (Figure S5). *Aip* was previously shown to be regulated by miR-34a[37] and was thus included (Figure 3A,D). miR-34a overexpression decreased *Gnai2* mRNA levels by about 30% vs nonspecific miRNA negative control transfected cells (Figure 3B); miR-34a downregulation increased *Gnai2* expression by about 1.5-fold (Figure 3E). No changes in *Gnai3* levels were observed after miR-34a modulation (Figure 3C,F).

Then, we tested whether miR-34a directly targets *Gnai2* using reporter gene assays. Given that a seed match for miR-34a in the 3'UTR region of rat *Gnai2* was predicted, we cloned this sequence into the psiCHECK-2 vector upstream of the firefly luciferase gene (Figure 3G). This construct was then transfected into HEK293 cells

FIGURE 2 mir-34a promotes tumorigenic behavior in PA cells. A-D, GH3 cells were transfected with an unspecific miRNA mimic (unspecific control) or with specific mimics for mature miR-34a or miR-145. All assays were performed 24 hours after transfection. The values are normalized against the negative control arbitrarily set to 100%. Results are reported as the mean ± SEM. A, Cell viability was assessed by the WST-1 assay. The experiment was independently performed three times each with six technical replicates. B, Migration assays were conducted using the Boyden chamber and the migrated cells were counted. The experiment was independently performed twice each time with three technical replicates. C, Transfected GH3 cells were plated and selected. Seven days later the colonies were fixed, stained and those that reached a diameter >100 μm were counted. The experiment was independently performed three times each with 3 to 4 technical replicates. D, Caspase 3/7 activity was measured to assess apoptosis. The experiment was independently performed three times each with two technical replicates. Results are reported as the mean ± SEM $^{*}P < .05$; $^{**}P < .01$; $^{***}P < .001$; n.s., not significant (by one-way ANOVA). E-G, effect of miR-34a and miR-145 on cell viability and GH or PRL secretion of GH3 cells following octreotide treatment. GH3 cells were transfected with an unspecific miRNA (unspecific control) or with specific mimics for mature miR-34a or miR-145 and subsequently treated with 10 nM octreotide (Oct) for 72 hours or 100 nM Oct for 48 hours. Cell viability (E) and GH (F) or PRL (G) secretion were then measured using the WST-1 assay (E) or ELISA (F,G), respectively. The experiments were independently performed three times each with six (e) or two (F, G) technical replicates. The values are normalized against the untreated unspecific control arbitrarily set to 100%. Results are reported as the mean ± SEM. $^{*}P < .05$; $^{**}P < .01$; $^{***}P < .001$; n.s., not significant (by two-way ANOVA). H-L, effect of miR-34a and miR-145 on cAMP levels and ERK1/2 activation. H, GH3 cells were transfected with an unspecific miRNA (unspecific control) or with specific mimics for mature miR-34a or miR-145. Intracellular cAMP levels were measured 24 hours after transfection. The experiment was independently performed five times each with two technical replicates. The values are normalized against the negative control arbitrarily set to 100%. Results are reported as the mean ± SEM. I, In samples parallel to (H), western blot was performed 24 hours after transfection using an anti-p-ERK-1/2 antibody and an anti-ERK-1/2 antibody. The blot shown is representative of 2 independent experiments with similar results. L, Ratio of the band intensities of the blots (n = 2) described in (H). Results are reported as the mean ± SEM. $^{***}P < .001$; n.s., not significant (by one-way ANOVA). UT, untransfected; UC, unspecific control

together with an unspecific miRNA inhibitor or the anti-miR-34a, and luciferase activity was monitored. A decrease in luciferase activity was detected between cells cotransfected with empty vector and unspecific control miRNA inhibitor vs cells cotransfected with empty vector and anti-miR-34a inhibitor (Figure 3I). In contrast, anti-miR-34a increased the luciferase activity of the construct containing the *Gnai2*

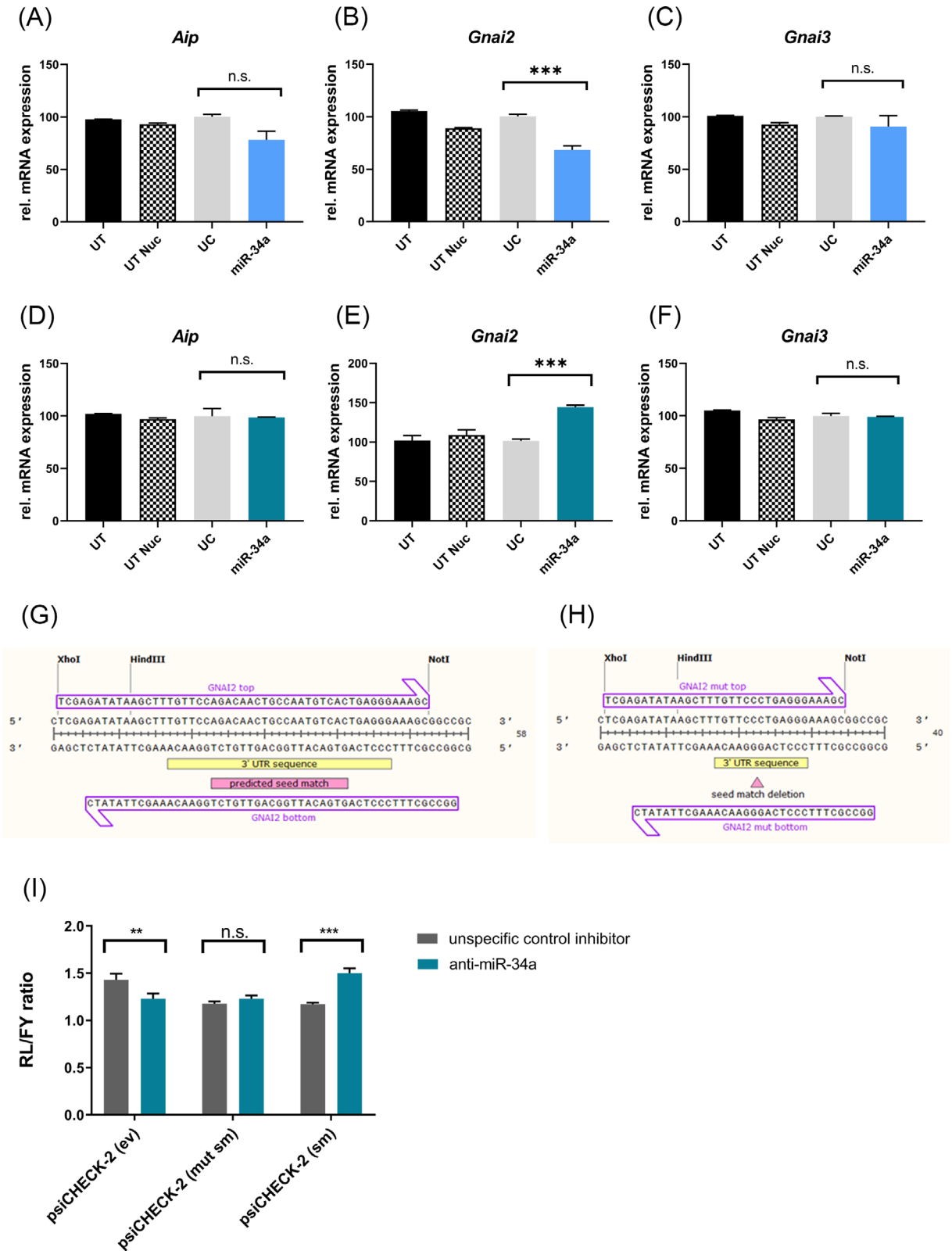

FIGURE 3 Legend on next page.

seed match *vs* unspecific miRNA inhibitor by almost 30% (Figure 3I). Deletion of the seed region abolished the anti-miR-34a-mediated regulation of luciferase activity, thereby confirming that this miRNA does bind to the seed sequence in *Gnai2* (Figure 3H,I).

3.8 | Gαi2 expression is reduced in human *AIP*mut + PAs

*AIP*mut+ PAs show an increase in miR-34a expression, which in turn regulates *Gnai2* expression. Thus, we next investigated Gαi2 (and AIP) expression by immunohistochemistry (IHC) on *AIP*mut− and *AIP*mut+ samples (Table S1). Slides were then scored semiquantitatively for staining intensity (Figure 4A). In total, 38 human PA tumors were scored for AIP expression and 30 (n = 18 *AIP*mut−; n = 12 *AIP*mut+) for Gαi2 expression (Figure 4B,C). We found that levels of Gαi2 were significantly lower in *AIP*mut+ *vs* *AIP*mut− tumors ($P < .05$; Figure 4D), whereas there was no statistically significant difference in AIP staining between the two sample groups (Figure 4E). By only considering the somatotropinomas (n = 13, *AIP*mut−; n = 9, *AIP*mut+), decreased Gαi2 staining in *AIP*mut + tumors was even more pronounced ($P < .01$; Figure 4F). Again, no significant difference in AIP expression was detected between *AIP*mut+ and *AIP*mut− somatotropinomas (Figure 4G). Not always tumors of *AIP*mut+ patients lacked AIP expression (Figure S6). A positive correlation between Gαi2 and AIP was found when all samples (*AIP*mut+ and *AIP*mut−) were analyzed together (Figure S7A). A detailed analysis of each group revealed that the positive correlation could only be observed in *AIP*mut− (Figure S7B), but not in *AIP*mut+ (Figure S7C) samples.

In *AIP*mut− PAs, invasive tumors have a lower expression score of both, AIP and Gαi2 (Figure S7A,C), whereas no difference in expression scores of either protein was seen in the *AIP*mut+ patient group (Figure S8).

4 | DISCUSSION

Acromegaly is a rare and disfiguring disease that, if inadequately treated, carries significant morbidity and increased mortality.[12] Resistance to medical therapy with SST2-specific SSAs like octreotide or lanreotide is an important impediment to hormonal control in acromegaly. *AIP*mut in acromegaly leads to such SSA resistance, which has a major clinical impact on patients as *AIP*mut are also associated with young-onset, large and invasive PAs.[10] The mechanisms to explain this phenotype are therefore of high clinical relevance. We report here for the first time that *AIP*mut+ somatotropinomas have a distinct miRNA profile of miR-34a upregulation, a well-known miRNA that can function as an oncomiR in multiple cancers. Loss of AIP due to mutation led to increased miR-34a, which was associated with increased cAMP and low Gαi2 expression. Importantly, miR-34a dysregulation also recapitulated the SSA-resistant phenotype of human *AIP*mut, with blunting of the antiproliferative and GH secretory effects of octreotide. This suggests that the aggressive and therapeutically-resistant features of *AIP*mut in PA could be mediated by dysregulated miR-34a.

Nine miRNAs were differentially expressed between *AIP*mut+ and *AIP*mut− somatotropinomas, five of which were validated by qRT-PCR: miR-187, miR-145, miR-34a, (upregulated in *AIP*mut+) and miR-195 (downregulated). Among the *AIP*mut+ PA samples we used, the missense mutation p.R271W was the most frequent and is a recurrent mutation clinically.[38] As p.R271W is known to affect *AIP* function,[39] we used this variant to verify the causal relationship between mutant *AIP* and miRNA expression by ectopically overexpressing AIP-R271W in *Aip*-deficient MEFs. AIP-R271W was present at much lower levels than wild-type AIP due to enhanced degradation in part through the proteasome. This accords with Hernandez-Ramirez et al who reported decreased stability of AIP-R271W in HEK293 cells.[30] Despite its short half-life, ectopic AIP-R271W promoted $AIP^{-/-}$ MEFs proliferation. This effect was accompanied by specific upregulation of miR-34a and miR-145, thereby establishing a relationship between *AIP*mut and expression of these two miRNAs.

In rat pituitary GH3 cells, upregulation of miR-34a promoted migration and inhibited apoptosis, whereas miR-145 moderately increased cell viability and decreased apoptosis. Furthermore, octreotide inhibited proliferation and GH secretion in GH3 cells, whereas, miR-34a overexpression counteracted this. Therefore, stimulation of miR-34a expression by mutant AIP leads to resistance to

FIGURE 3 miR-34a directly targets *Gnai2* in GH3 cells. GH3 cells were just pulsed without DNA, or transfected with an unspecific miRNA (unspecific control), with a specific mimic for mature miR-34a (A-C) or with an antagonist of miR-34a (D-F). mRNA levels of *Aip* (A, D), *Gnai2* (B, E), or *Gnai3* (C, F) were determined 24 hours after transfection by qRT-PCR. Each amplification was independently performed 3 to 6 times each with two technical replicates. The values are normalized against the unspecific control arbitrarily set to 100%. Results are reported as the mean ± SEM. ***$P < .001$; n.s., not significant (by one-way ANOVA). G, Sequence of the DNA fragment cloned into the psiCHECK-2 luciferase vector (*GNAI2* oligos) which contains the predicted seed match of miR-34a (pink) located in the 3′ UTR of the rat *Gnai2* gene (yellow). H, Sequence of the DNA fragment cloned into the psiCHECK-2 luciferase vector (*GNAI2* oligos) which contains a deletion of the predicted seed match of miR-34a (pink) in the 3′ UTR of the rat *Gnai2* gene (yellow). I, HEK293 cells were co-transfected with the empty vector and an unspecific miRNA inhibitor (unspecific control inhibitor) or a specific antagonist for miR-34a (anti-miR34a), with the seed match-containing vector (shown in a) and either the unspecific miRNA or the specific anti-miR34a or with the mutated seed match-containing vector (shown in b) with the unspecific miRNA or the specific anti-miR34a. The experiment was independently performed three times each with three technical replicates. The values are normalized against an untransfected control (not shown in the graph). Results are reported as the mean ± SEM. **$P < .01$; ***$P < .001$; n.s., not significant (by two-way ANOVA). UT, untransfected; UT Nuc, untransfected Nucleofector; UC, unspecific control; ev, empty vector; sm, seed match; mut sm, mutated seed match

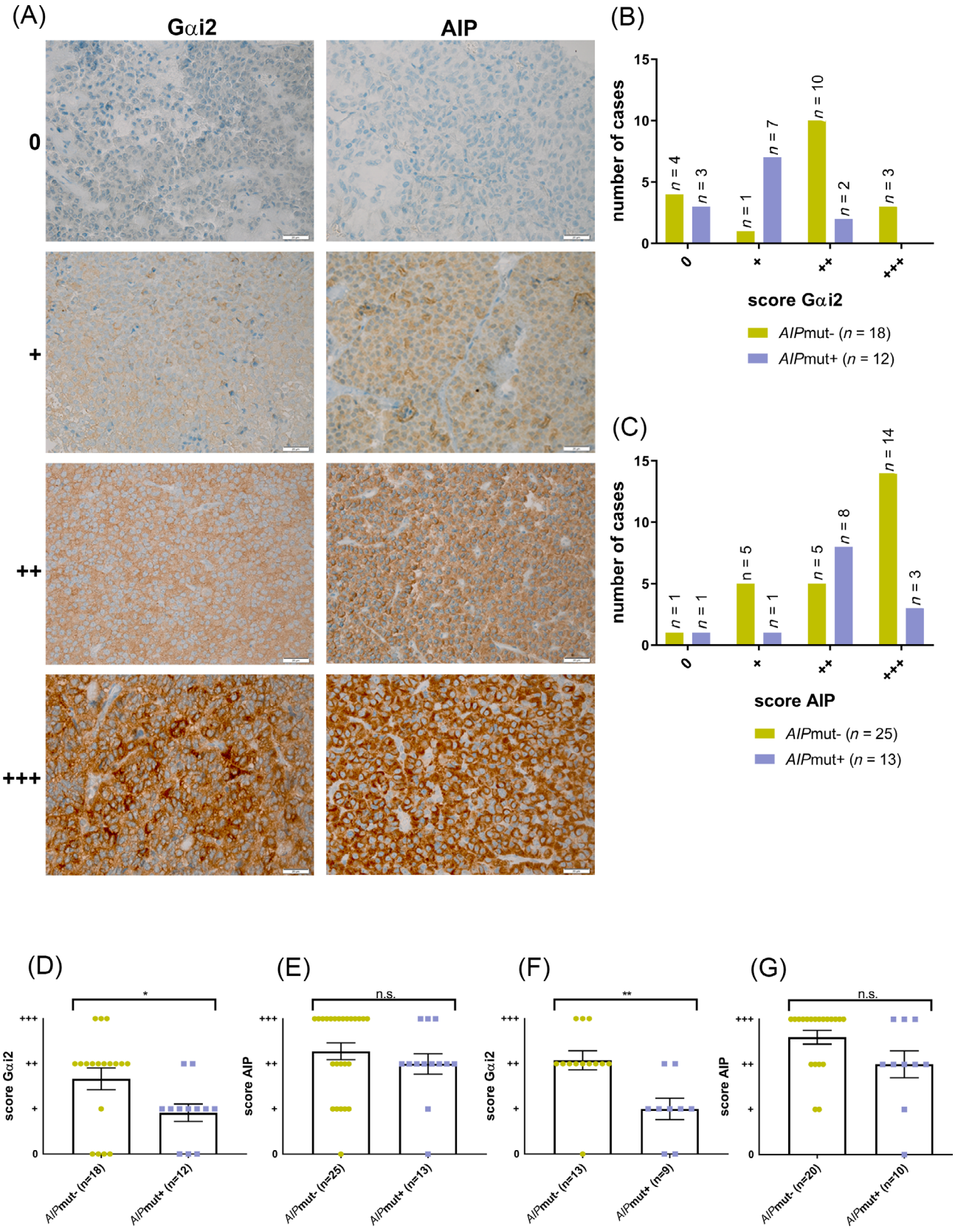

FIGURE 4 Gαi2 expression levels are reduced in in human AIPmut + PAs. A, Immunohistochemical staining of four representative primary PAs for Gαi2 and AIP. The samples cover the range of staining intensities observed (0; +; ++; +++). Antibodies anti-Gαi2 (1/200) and anti-AIP (1/1000) were used. Original magnification: ×200; scale bar = 20 μm. B,C, Staining intensities of the samples that could be scored for Gαi2 (B, n = 30) or AIP (C, n = 38). Samples are divided in AIPmut− and AIPmut+ PAs. Expression of AIP and Gαi2 in human AIPmut− and AIPmut+ PAs. D-E, Gαi2 (D) and AIP (E) staining intensities in AIPmut− and AIPmut+ samples. F-G, Gαi2 (F) and AIP (G) staining intensities in AIPmut− and AIPmut+ somatotropinomas. Results are reported as the mean ± SEM. *$P < .05$; **$P < .01$; n.s., not significant (by unpaired two-tailed Student's *t*-test)

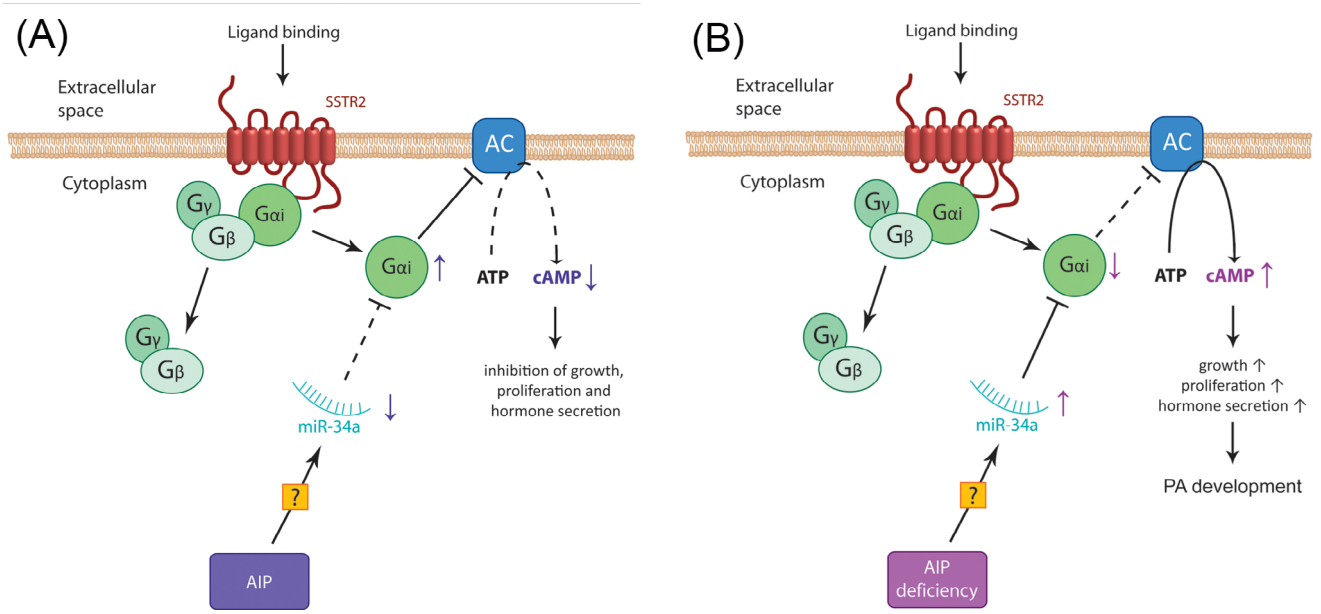

FIGURE 5 Model of the effect of AIP deficiency on intracellular processes. A, Physiological and B, pathological (AIP mutation or loss) scenario in which AIP deficiency leads to upregulation of miR-34a which in turn decreases Gαi2 levels. The inhibition of AC by Gαi2 is reduces and the AC produces nonphysiological amounts of cAMP, which acts as an mitogenic signal in the cell

octreotide treatment, thereby recapitulating the clinical phenotype of *AIP*mut+ PA patients.

Both miR-34a and miR-145 have been implicated in various human tumors. miR-145 is co-transcribed with miR-143 and both have been described as a tumor suppressive miRNAs in corticotropinomas and craniopharyngioma.[22,40] In PAs, mir-145 inhibits mTOR signaling in invasive tumors, sensitizes prolactinoma cells to bromocriptine, is downregulated in invasive NFPAs and its overexpression reduces proliferation and invasion of NFPA cells in vitro.[23,41,42] miR-145 can, however, also foster tumor development: knockout of the miR-143/miR-145 cluster reduced tumor number and tumor area, and increased angiogenesis in a lung cancer mouse model.[43]

miR-34a, together with miR-34b and miR-34c, are transcriptionally regulated by p53. miR-34a was initially considered a tumor suppressor since it is downregulated in several cancers, and reduces proliferation and induces apoptosis of tumor cells.[40,44,45] However, recent evidence also points to a pro-oncogenic role for miR-34a as it is overexpressed in gastric cancer and brain tumors, among others.[46-48] miR-34a plays a proproliferative and antiapoptotic role in vascular and lymphoid tissues,[49-51] and it was also found to induce chemoresistance of osteosarcoma cells,[52] and to promote genomic instability.[53] Therefore, miR-34a overexpression, a feature often acquired during carcinogenesis, can play an oncogenic or tumor-suppressive role in a tissue- and context-specific manner. In the normal pituitary, miR-34a is expressed at a level similar to that seen in AIPmut− somatotropinomas, being overexpressed only in adenomas with an *AIP* mutation (Figure S9). Interestingly, miR-34a was previously shown to have increased expression in non-AIPmut somatotropinomas with low AIP protein levels, and to directly target and inhibit *AIP* in a nonpituitary model (HEK293).[37] While Denes et al[37] found only a modest effect of increased miR-34a on Aip protein levels in GH3 cells, we have expanded this to show that *AIP*mut in PAs specifically upregulates miR-34a, where it functions as an oncomiR.

In contrast to findings from our group and from Denes et al,[37] it was recently reported that long-term overexpression of miR-34a decreases the proliferation of GH4C1 cells,[54] a clone derived from GH3 cells but that produces negligible amounts of GH. We did not see changes in GH4C1 cell proliferation upon overexpression of miR-34a up to 72 hours posttransfection (Figure S10) whereas in GH3 cells an increase in viability was already detectable 24 hours post-transfection and lasted for several days (eg, in clonogenic assays). This discrepancy suggests that miR-34a elicits different effects due to underlying secretory and molecular heterogeneity between GH3 and GH4C1 clones.[55,56]

Dysregulation of intracellular cAMP levels is a hallmark of functioning endocrine tumors, including somatotropinomas, where cAMP promotes cell division and GH secretion. A link between AIP and cAMP has been established in that overexpression of wild-type AIP in GH3 cells attenuates the forskolin-dependent increase in intracellular cAMP and GH secretion, whereas silencing of endogenous *Aip* increases cAMP concentration.[33] Mechanistically, AIP interacts with several members of the cAMP signaling cascade, including phosphodiesterases, the enzymes that deactivate cAMP, and G proteins, which can either activate AC and increase cAMP (activating) or have the opposite effects (inhibitory).[16,57] In *Aip*-deficient MEFs, the inhibitory Gαi2 and Gαi3 proteins do not inhibit cAMP synthesis, which suggests that *AIP*mut-related pituitary tumorigenesis may occur via Gαi signaling and cAMP.[17] In this context, our finding that in PA cells *AIP*mut leads to upregulation of miR-34a, which in turn increases intracellular cAMP levels, offers an additional molecular mechanism relating defective *AIP* to cAMP production (Figure 5). Among the predicted miR-34a

targets was *GNAI2* encoding Gαi2, which was confirmed to be a direct target by reporter gene assays. Accordingly, miR-34a overexpression in PA cells reduces *GNAI2* levels, while its downregulation increases them. A reduction intracellular levels of Gαi2 is expected to enhance AC activity and to increase cAMP levels, which we observed. Although a role has been suggested for Gαi2 in mediating the effects of defective *Aip*, the mechanism was unknown as loss-of-function mutations in *GNAI* genes are not seen in PAs.[58] We demonstrate that *AIP*mut decreases *GNAI2* expression via miR-34a upregulation, and this ultimately leads to increased AC activity as well as cAMP levels (Figure 5).

In line with previous reports, we observed a trend towards a negative correlation between AIP levels and tumor size.[59,60] Also, we confirmed that low AIP staining is associated with higher likelihood of tumor invasion and *AIP*mut+ status did not predict AIP staining intensity.[61] We also found that *AIP*mut are associated with a reduction in Gαi2 levels, thereby extending the findings of Tuominen et al.[17] Similar to AIP, the levels of Gαi2 are reduced in invasive vs noninvasive PAs only in the *AIP*mut+ group.

In summary, we show that *AIP*mut in GH-secreting PAs leads to dysregulation of a specific subset of miRNAs, including miR-34a, which is induced by *AIP*mut and has pro-oncogenic functions in somatotropinomas through regulation of Gαi2 expression and increased cAMP concentrations. As increased levels of miR-34a impair the response of PA cells to octreotide, the lack of response of *AIP*mut+ patients to first-generation SSAs might be mediated by induction of miR-34a expression. These findings further support the hypothesis that failure to inhibit cAMP synthesis due to downregulation of Gαi2 is key event in AIP-mediated pituitary tumorigenesis. Furthermore, this adds another level of complication to the multifaceted role of AIP in PAs given that the increase of miR-34a may lead to the regulation of other genes in addition to *Gnai2*. As both high miR-34a and low Gαi2 levels are associated with resistance to SSA therapy, they represent potential biomarkers that could be used as evidence to personalize treatment choices and improve outcomes in *AIP*mut patients.

ACKNOWLEDGEMENTS

The authors thank E. Pulz for excellent technical assistance; Dr S. Molatore for advice and Prof. S. Herzig for scientific support. We thank the patients whose participation made our study possible. This work was supported by the Deutsche Forschungsgemeinschaft (DFG) within the CRC/Transregio 205/1 (subproject B11), by the Deutsche Krebshilfe (grant 70112383), by the Fonds d'Investissement Pour la Recherche Scientifique (FIRS) 2014-2018, CHU de Liège and by a grant from the JABBS Foundation, UK. This work was partially supported by the Helmholtz Alliance "Aging and Metabolic Programming, AMPro" (to J. B.). Open access funding enabled and organized by Projekt DEAL.

CONFLICT OF INTEREST

The authors declare that there is no conflict of interest that could be perceived as prejudicing the impartiality of the research reported.

DATA AVAILABILITY STATEMENT

The array data are openly available in GEO (GSE140604). All other data will be made available upon reasonable request.

ETHICS STATEMENT

These studies were approved by the local ethics committees and prior to surgery, all patients signed a written informed consent.

ORCID

Natalia S. Pellegata https://orcid.org/0000-0002-8000-7784

REFERENCES

1. Ostrom QT, Gittleman H, Truitt G, Boscia A, Kruchko C, Barnholtz-Sloan JS. CBTRUS statistical report: primary brain and other central nervous system tumors diagnosed in the United States in 2011–2015. *Neuro Oncol*. 2018;20:iv1-iv86.
2. Daly AF, Rixhon M, Adam C, Dempegioti A, Tichomirowa MA, Beckers A. High prevalence of pituitary adenomas: a cross-sectional study in the province of Liège, Belgium. *J Clin Endocrinol Metab*. 2006; 91:4769-4775.
3. Casanueva FF, Barkan AL, Buchfelder M, et al. Criteria for the definition of pituitary tumor centers of excellence (PTCOE): a pituitary society Statement. *Pituitary*. 2017;20:489-498.
4. Daly AF, Beckers A. Chapter 21—genetics of pituitary tumor syndromes. *The Pituitary*. Amsterdam: Elseiver; 2017:619-630.
5. Daly AF, Jaffrain-Rea M-L, Ciccarelli A, et al. Clinical characterization of familial isolated pituitary adenomas. *J Clin Endocrinol Metab*. 2006; 91:3316-3323.
6. Trivellin G, Daly AF, Faucz FR, et al. Gigantism and acromegaly due to Xq26 microduplications and GPR101 mutation. *N Engl J Med*. 2014; 371:2363-2374.
7. Wise-Oringer BK, Zanazzi GJ, Gordon RJ, et al. Familial X-linked Acrogigantism: postnatal outcomes and tumor pathology in a prenatally diagnosed infant and his mother. *J Clin Endocrinol Metab*. 2019; 104:4667-4675.
8. Vierimaa O, Georgitsi M, Lehtonen R, et al. Pituitary adenoma predisposition caused by germline mutations in the AIP gene. *Science (80-)*. 2006;312:1228-1230.
9. Daly AF, Vanbellinghen J-F, Sok KK, et al. Aryl hydrocarbon receptor-interacting protein gene mutations in familial isolated pituitary adenomas: analysis in 73 families. *J Clin Endocrinol Metab*. 2007;92:1891-1896.
10. Daly AF, Tichomirowa MA, Petrossians P, et al. Clinical characteristics and therapeutic responses in patients with germ-line AIP mutations and pituitary adenomas: an international collaborative study. *J Clin Endocrinol Metab*. 2010;95:E373-E383.
11. Buchfelder M, Schlaffer S. The surgical treatment of acromegaly. *Pituitary*. 2017;20:76-83.
12. Katznelson L, Laws ER, Melmed S, et al. Acromegaly: an Endocrine Society clinical practice guideline. *J Clin Endocrinol Metab*. 2014;99: 3933-3951.
13. Fuentes-Fayos AC, García-Martínez A, Herrera-Martínez AD, et al. Molecular determinants of the response to medical treatment of growth hormone secreting pituitary neuroendocrine tumors. *Minerva Endocrinol*. 2019;44:109-128.
14. Igreja S, Chahal HS, King P, et al. Characterization of aryl hydrocarbon receptor interacting protein (AIP) mutations in familial isolated pituitary adenoma families. *Hum Mutat*. 2010;31:950-960.
15. Schernthaner-Reiter MH, Trivellin G, Stratakis CA. Interaction of AIP with protein kinase a (cAMP-dependent protein kinase). *Hum Mol Genet*. 2018;27:2604-2613.
16. Bolger GB, Bizzi MF, Pinheiro SV, et al. cAMP-specific PDE4 phosphodiesterases and AIP in the pathogenesis of pituitary tumors. *Endocr Relat Cancer*. 2016;23:419-431.

17. Tuominen I, Heliövaara E, Raitila A, et al. AIP inactivation leads to pituitary tumorigenesis through defective Gαi-cAMP signaling. *Oncogene*. 2015;34:1174-1184.
18. Ritvonen E, Pitkänen E, Karppinen A, et al. Impact of AIP and inhibitory G protein alpha 2 proteins on clinical features of sporadic GH-secreting pituitary adenomas. *Eur J Endocrinol*. 2017;176:243-252.
19. Bottoni A, Zatelli MC, Ferracin M, et al. Identification of differentially expressed microRNAs by microarray: a possible role for microRNA genes in pituitary adenomas. *J Cell Physiol*. 2007;377:370-377.
20. Bottoni A, Piccin D, Tagliati F, Luchin A, Zatelli MC, degli Uberti EC. miR-15a and miR-16-1 down-regulation in pituitary adenomas. *J Cell Physiol*. 2005;204:280-285.
21. Butz H, Liko I, Czirjak S, et al. MicroRNA profile indicates downregulation of the TGFβ pathway in sporadic non-functioning pituitary adenomas. *Pituitary*. 2011;14:112-124.
22. Amaral FC, Torres N, Saggioro F, et al. MicroRNAs differentially expressed in ACTH-secreting pituitary tumors. *J Clin Endocrinol Metab*. 2009;94:320-323.
23. Jian M, Du Q, Zhu D, et al. Tumor suppressor miR-145-5p sensitizes prolactinoma to bromocriptine by downregulating TPT1. *J Endocrinol Invest*. 2019;42:639-652.
24. Mao ZG, He DS, Zhou J, et al. Differential expression of microRNAs in GH-secreting pituitary adenomas. *Diagn Pathol*. 2010;5:79.
25. Trivellin G, Butz H, Delhove J, et al. MicroRNA miR-107 is overexpressed in pituitary adenomas and inhibits the expression of aryl hydrocarbon receptor-interacting protein in vitro. *Am J Physiol Endocrinol Metab*. 2012;303:E708-E719.
26. Rainer J, Sanchez-Cabo F, Stocker G, Sturn A, Trajanoski Z. CARMAweb: comprehensive R- and bioconductor-based web service for microarray data analysis. *Nucleic Acids Res*. 2006;34:W498-W503.
27. Molatore S, Liyanarachchi S, Irmler M, et al. Pheochromocytoma in rats with multiple endocrine neoplasia (MENX) shares gene expression patterns with human pheochromocytoma. *Proc Natl Acad Sci U S A*. 2010;107:18493-18498.
28. Molatore S, Marinoni I, Lee M, et al. A novel germline CDKN1B mutation causing multiple endocrine tumors: clinical, genetic and functional characterization. *Hum Mutat*. 2010;31:E1825-E1835.
29. Yu C, Li J, Sun F, Cui J, Fang H, Sui G. Expression and clinical significance of miR-26a and pleomorphic adenoma gene 1 (PLAG1) in invasive pituitary adenoma. *Med Sci Monit*. 2016;22:5101-5108.
30. Hernández-Ramírez LC, Martucci F, Morgan RML, et al. Rapid proteasomal degradation of mutant proteins is the primary mechanism leading to tumorigenesis in patients with missense AIP mutations. *J Clin Endocrinol Metab*. 2016;101:3144-3154.
31. Cheung NW, Boyages SC. Somatostatin-14 and its analog octreotide exert a cytostatic effect on GH3 rat pituitary tumor cell proliferation via a transient G0/G1 cell cycle block. *Endocrinology*. 1995;136:4174-4181.
32. Gruszka A, Ren S-G, Dong J, Culler MD, Melmed S. Regulation of growth hormone and prolactin gene expression and secretion by chimeric somatostatin-dopamine molecules. *Endocrinology*. 2007;148:6107-6114.
33. Formosa R, Xuereb-Anastasi A, Vassallo J. AIP regulates cAMP signalling and growth hormone secretion in GH3 cells. *Endocrine-Related*. 2013;20:495-505.
34. Vallar L, Spada A, Giannattasio G. Altered Gs and adenylate cyclase activity in human GH-secreting pituitary adenomas. *Nature*. 1987;330:566-568.
35. Lania A, Filopanti M, Corbetta S, et al. Effects of hypothalamic neuropeptides on extracellular signal-regulated kinase (ERK1 and ERK2) cascade in human tumoral pituitary cells. *J Clin Endocrinol Metab*. 2003;88:1692-1696.
36. Pertuit M, Barlier A, Enjalbert A, Gérard C. Signalling pathway alterations in pituitary adenomas: involvement of Gsalpha, cAMP and mitogen-activated protein kinases. *J Neuroendocrinol*. 2009;21:869-877.
37. Dénes J, Kasuki L, Trivellin G, et al. Regulation of aryl hydrocarbon receptor interacting protein (AIP) protein expression by MiR-34a in sporadic somatotropinomas. *PLoS One*. 2015;10:e0117107.
38. Beckers A, Aaltonen LA, Daly AF, Karhu A. Familial isolated pituitary adenomas (FIPA) and the pituitary adenoma predisposition due to mutations in the aryl hydrocarbon receptor interacting protein (AIP) gene. *Endocr Rev*. 2013;34:239-277.
39. Bell DR, Poland A. Binding of aryl hydrocarbon receptor (AhR) to AhR-interacting protein. The role of hsp90. *J Biol Chem*. 2000;275:36407-36414.
40. Campanini ML, Colli LM, Paixao BM, et al. CTNNB1 gene mutations, pituitary transcription factors, and MicroRNA expression involvement in the pathogenesis of adamantinomatous craniopharyngiomas. *Horm Cancer*. 2010;1:187-196.
41. Zhou K, Fan YD, Wu PF, et al. MicroRNA-145 inhibits the activation of the mTOR signaling pathway to suppress the proliferation and invasion of invasive pituitary adenoma cells by targeting AKT3 in vivo and in vitro. *Onco Targets Ther*. 2017;10:1625-1635.
42. Du Q, Hu B, Feng Y, et al. circOMA1-mediated miR-145-5p suppresses tumor growth of nonfunctioning pituitary adenomas by targeting TPT1. *J Clin Endocrinol Metab*. 2019;104:2419-2434.
43. Dimitrova N, Gocheva V, Bhutkar A, et al. Stromal expression of miR-143/145 promotes Neoangiogenesis in lung cancer development. *Cancer Discov*. 2016;6:188-201.
44. Wang JX, Zhang QJ, Pei SG, Yang BL. Effect and mechanism of miR-34a on proliferation, apoptosis and invasion of laryngeal carcinoma cells. *Asian Pac J Trop Med*. 2016;9:494-498.
45. Deng X, Zheng H, Li D, et al. MicroRNA-34a regulates proliferation and apoptosis of gastric cancer cells by targeting silent information regulator 1. *Exp Ther Med*. 2018;15:3705-3714.
46. Braoudaki M, Lambrou GI, Giannikou K, et al. Microrna expression signatures predict patient progression and disease outcome in pediatric embryonal central nervous system neoplasms. *J Hematol Oncol*. 2014;7:96.
47. Ruiz Esparza-Garrido R, Velazquez-Flores MA, Diegoperez-Ramirez J, et al. A proteomic approach of pediatric astrocytomas: MiRNAs and network insight. *J Proteomics*. 2013;94:162-175.
48. Ferretti E, De Smaele E, Po A, et al. MicroRNA profiling in human medulloblastoma. *Int J Cancer*. 2009;124:568-577.
49. Wang P, Xu J, Hou Z, et al. miRNA-34a promotes proliferation of human pulmonary artery smooth muscle cells by targeting PDGFRA. *Cell Prolif*. 2016;49:484-493.
50. Sotillo E, Laver T, Mellert H, et al. Myc overexpression brings out unexpected antiapoptotic effects of miR-34a. *Oncogene*. 2011;30:2587-2594.
51. Rizzo M, Mariani L, Cavallini S, Simili M, Rainaldi G. The overexpression of miR-34a fails to block DoHH2 lymphoma cell proliferation by reducing p53 via c-MYC down-regulation. *Nucleic Acid Ther*. 2012;22:283-288.
52. Pu Y, Zhao F, Li Y, et al. The miR-34a-5p promotes the multichemoresistance of osteosarcoma via repression of the AGTR1 gene. *BMC Cancer*. 2017;17:45.
53. Krause CJ, Popp O, Thirunarayanan N, Dittmar G, Lipp M, Muller G. MicroRNA-34a promotes genomic instability by a broad suppression of genome maintenance mechanisms downstream of the oncogene KSHV-VGPCR. *Oncotarget*. 2016;7:10414-10432.
54. Yang Z, Zhang T, Wang Q, Gao H. Overexpression of microRNA-34a attenuates proliferation and induces apoptosis in pituitary adenoma cells via SOX7. *Mol Ther Oncolytics*. 2018;10:40-47.
55. Castillo AI, Aranda A. Differential regulation of pituitary-specific gene expression by insulin-like growth factor 1 in rat pituitary GH4C1 and GH3 cells*. *Endocrinology*. 1997;138:5442-5451.

56. Tagliati F, Gagliano T, Gentilin E, et al. Magmas overexpression inhibits staurosporine induced apoptosis in rat pituitary adenoma cell lines. *PLoS One*. 2013;8:e75194.
57. de Oliveira SK, Hoffmeister M, Gambaryan S, Muller-Esterl W, Guimaraes JA, Smolenski AP. Phosphodiesterase 2A forms a complex with the co-chaperone XAP2 and regulates nuclear translocation of the aryl hydrocarbon receptor. *J Biol Chem*. 2007;282:13656-13663.
58. Demir H, Donner I, Kivipelto L, et al. Mutation analysis of inhibitory guanine nucleotide binding protein alpha (GNAI) loci in young and familial pituitary adenomas. *PLoS One*. 2014;9:e109897.
59. Kasuki Jomori de Pinho L, Vieira Neto L, Armondi Wildemberg LE, et al. Low aryl hydrocarbon receptor-interacting protein expression is a better marker of invasiveness in somatotropinomas than Ki-67 and p53. *Neuroendocrinology*. 2011;94:39-48.
60. Daly AF, Cano DA, Venegas-Moreno E, et al. Aip and men1 mutations and aip immunohistochemistry in pituitary adenomas in a tertiary referral center. *Endocr Connect*. 2019;8:338-348.
61. Jaffrain-Rea M-L, Angelini M, Gargano D, et al. Expression of aryl hydrocarbon receptor (AHR) and AHR-interacting protein in pituitary adenomas: pathological and clinical implications. *Endocr Relat Cancer*. 2009;16:1029-1043.

SUPPORTING INFORMATION

Additional supporting information may be found online in the Supporting Information section at the end of this article.

How to cite this article: Bogner E-M, Daly AF, Gulde S, et al. miR-34a is upregulated in *AIP*-mutated somatotropinomas and promotes octreotide resistance. *Int. J. Cancer*. 2020;147:3523–3538. https://doi.org/10.1002/ijc.33268